Wind-plus-Battery System Optimisation for Frequency Response Service: The UK Perspective

Fulin Fan, Giorgio Zorzi, David Campos-Gaona
Dept. Electronic and Electrical Engineering
University of Strathclyde
Glasgow, United Kingdom
f.fan;giorgio.zorzi;d.campos-gaona@strath.ac.uk

John Nwobu
Offshore Renewable Energy Catapult
Glasgow, United Kingdom
john.nwobu@ore.catapult.org.uk

***Abstract*--Battery energy storage systems (BESSs) co-located with wind farms (WFs) can provide frequency response (FR) services to AC grids exploiting the existing connection points. The UK FR market reforms introduce the Dynamic Low High (DLH) product that is procured by 4-hourly blocks in weekly auctions. This paper develops a modelling framework to optimise the BESS size along with bidding and operating strategies of a co-location system for the DLH provision based on the UK perspective. Power flows across the system are dispatched by the designed strategies, and employed to estimate the system's net present value which is then maximised to suggest the best BESS size, state of charge levels for the DLH delivery and WF-BESS interaction, as well as the DLH capacity and 4-hourly blocks to be bid for in weekly auctions. The optimisation results are compared between different strategies and discussed around the feasibility of co-location projects under new circumstances.**

***Index Terms*—Battery energy storage sizing, co-location system, Dynamic Low High, operating strategy, UK perspective.**

NOMENCLATURE

Δt	Time step length.
j, m	Settlement period (SP) or calendar month index.
EFA	Electricity forward agreement.
e, w	Service day or week index.
$N_{\Delta t}$	Number of time steps before next EFA block.
DLH	Dynamic Low High.
EFA_u	First untendered EFA block.
N_{EFA}^{max}	Number of consecutive tendered EFA blocks.
$P_{w,e}^{DLH}$	DLH contracted power capacity.
P_{req}^{DLH}	Required DLH response.
PPM	Percentage Performance Measure.
K_w	Weekly DLH performance factor.
$A_{w,e,j}$	Availability of DLH service in a SP.
$H_{w,e}$	Number of hours available for DLH service.
P_C	Connection point ampacity of wind farm (WF).
P_{WF}^{tot}	Available wind power output.
P_{WF}^{sell}	Wind power sold to grid across WF meter.
P_{WF}^{DLH}	Low-frequency response of WF.
P_{WF}^{str}	Wind power stored by battery storage.
P_{WF}^{curt}	Wind power curtailment.
BESS	Battery energy storage system.
AdC	Converter between WF and BESS.
C_B^R, C_B^{rm}	Rated or remaining BESS energy capacity.
P_B^R, P_A^R	Rated power capacity of BESS or AdC.
η	Power conversion efficiency.
P_B^{DLH}	BESS power output across DLH meter.
P_B^{sell}	BESS export to AC grid across WF meter.
SOC_{op}	Optimal state of charge (SOC) level.
SOC_{ch}, SOC_{dl}	SOC limit related to P_{WF}^{str} or P_B^{sell}.
SOC_o, SOC_n	SOC level at the start or end of a time step.
SOC_t	SOC level after delivery of P_B^{DLH}.
$\overline{SOC}$, $\underline{SOC}$	Maximum or minimum allowable SOC.
NPV	Net present value.
R, C, δ	Revenue, cost, or change after co-location.
$\mathcal{P}$	Unit price in £/MWh or £/MW/h.
CAPEX	Capital expenditure.
OPEX	Operational expense.
TNUoS	Transmission Network Use of System.
BSUoS	Balancing Services Use of System.
RO	Renewables Obligation.
EIC	Energy imbalance charge.

I. INTRODUCTION

Battery energy storage systems (BESSs) are considered key components in the transition to a low carbon, more flexible and more decentralised energy system [1]. The accelerated growth of BESSs and the rapid development of battery technologies in recent years [2] have led to the increasingly attractive option of co-locating a BESS within a renewable power plant [3] such as a wind farm (WF), forming a WF+BESS system. A co-located BESS not only helps manage the intermittent nature of wind generation [4], [5] but can also deliver ancillary services [5], [6] via the connection point of the WF, making the most efficient use of the existing infrastructure. The fast responses for both export and import of a BESS make it the suitable candidate for providing frequency response (FR) services that help balancing generation and demand to keep the grid frequency closer to the nominal level [7]. To offset the system inertia reduction caused by the increased renewable generation in the UK, the National

Submitted to the 22nd Power Systems Computation Conference (PSCC 2022).

Grid Electricity System Operator (NGESO) has been reforming the FR market by developing fast-acting products and procuring them closer to real time [8], [9]. An interim product introduced in November 2019 is Dynamic Low High (DLH) [10] which is a standardised version of the dynamic firm FR (FFR). Part of the monthly tendered FFR volume has been transferred to DLH and procured by 4-hourly electricity forward agreement (EFA) blocks via weekly auctions that intend to be trialled for 2 years to test closer-to-real-time procurement [9]. The UK FR market reforms drive the need of evaluating the technical and economic feasibility of a WF+BESS project and optimising the size and operating strategy of a co-located BESS in new circumstances.

Most research related to the energy storage system (ESS) optimisation for frequency regulation can be categorised into two main groups: (i) those estimate the minimum ESS size to keep the grid frequency stability given an expected penetration level of renewables [11]-[15]; and (ii) those address a trade-off in the ESS capacity and/or operating strategies between the ESS investment and the FR availability performance or payment [6], [16]-[21]. Considering severe contingencies of generation/load losses on a grid with different penetration levels of renewables, the BESS capacity was determined to achieve the target system inertia and power-to-frequency characteristics [11] or to satisfy a pre-defined frequency deviation criterion conditioning on the disturbance occurrences [12]. The size and costs of the BESS coordinating with demand side response to avoid the frequency limit violations were jointly minimised in [13]. References [14] and [15] also optimised the (hybrid) ESS sizes to help keeping the frequency deviations within the required limits but from the perspective of the frequency domain. From the perspective of an economic optimisation, the capacity and operating strategies of the BESS for the FR provision were optimised in [6] and [16] to maximise the expected net profit of the project considering the FR service payment and BESS costs. Instead of employing the exact FR service price issued in the market, a penalty for an inappropriate state of charge (SOC) causing a risk to the FR provision could be formulated in the optimisation problem [17]. Taking the UK FFR market or the PJM regulation market into account, reference [18] or [19] optimised operating and bidding strategies for BESS providers in the FR auctions, suggesting the minimum tender price and energy offset interval duration [18] or the highest contracted FR capacity possible while ensuring the required performance [19], respectively. In addition to FR payments, using ESSs to stack additional revenue streams were explored in literatures such as those from green subsidies [6] and electricity markets [16], [20].

Compared with a stand-alone ESS [18]-[20], co-locating the ESS with renewable energy sources such as WFs for frequency regulation has received an increased attention due either to the reduced ESS connection cost by sharing an existing connection point [6] or to the time shift of renewable generation and/or the power/energy reserve enabled by the ESS [15], [17], [21]-[23]. However, these research mostly focuses on using the co-located ESS to assist WFs in the FR delivery and allow WFs to generate close to their available power, rather than a direct use of the co-located ESS for the FR provision which is worth investigating in the ESS-friendly reform of the UK FR market [8]. This paper will develop a modelling framework to optimise the capacity of a co-located Li-Ion BESS along with bidding and operating strategies of a WF+BESS system for the DLH provision from the perspective of a transmission-connected WF owner, taking into account the latest information in the UK FR service market. In addition to the FR availability payment and BESS costs that are generally simulated for the BESS sizing [16]-[18], [21], the paper models the effects that the co-located BESS has on green subsidies, energy imbalance charges and connection charges based on the UK perspective. The net present value of the co-location system is computed until the energy capacity loss of the BESS exceeds a certain level, and then maximised by the particle swarm optimisation (PSO) algorithm to optimise the BESS size, SOC levels for the BESS energy restoration and the WF-BESS interaction as well as the DLH capacity and 4-hourly EFA blocks that should be bid for in weekly auctions. The main contributions of the paper include (i) the development of a DLH bidding strategy for energy-limited units; (ii) different designs in operating strategies between tendered and untendered EFA blocks which ensure the DLH performance and also reduce the wind curtailment; and (iii) a modelling framework for the BESS optimisation which can be adapted to the upcoming FR services, showing WF owners the profitability of co-location systems for the FR provision under the new UK FR market.

The paper is structured as follows: Section II describes the DLH service and designs bidding and operating strategies for a co-location system; Section III models costs and revenues of a co-location system and implements the PSO algorithm; Section IV discusses the optimisation results and the feasibility of a co-location system; and conclusions are presented in Section V.

II. Bidding and Operating Strategies for DLH

A. Dynamic Low High (DLH) Service

1) Technical requirements

The DLH service is a standardised version of dynamic FFR, delivering equal capacity of low (primary and secondary) and high FR [10]. The symmetrical characteristic of DLH is shown in Fig. 1, where it can be noted how the DLH response is zero whilst inside the deadband and varies symmetrically with the frequency outside the deadband [10]. Instead of an indefinite timescale for high FR in FFR, a DLH provider is required to sustain both low and high FR for 30 minutes only [10], which encourages energy-limited assets to bid for the DLH provision.

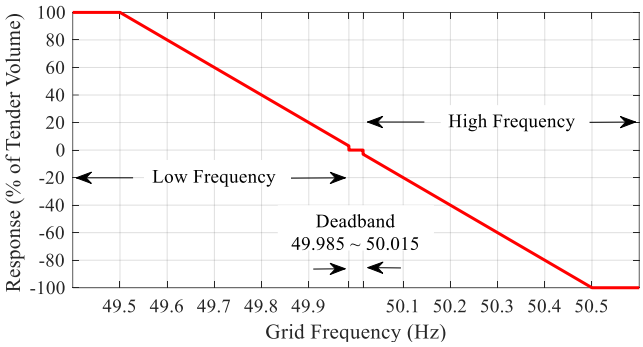

Fig. 1. Frequency response curve for the DLH service.

2) Availablity payment mechanisms

The DLH availability payment R_w^{DLH} (£) for the w^{th} service week is estimated by the market clearing price $\mathcal{P}_{w,e}^{DLH}$ (£/MW/h), contracted DLH capacity $P_{w,e}^{DLH}$ (MW) and available hours $H_{w,e}$ (h) in the e^{th} EFA block combined with a performance factor K_w for the week [10]:

$$R_w^{DLH} = \left(\sum_e \mathcal{P}_{w,e}^{DLH} \cdot P_{w,e}^{DLH} \cdot H_{w,e}\right) \cdot K_w \quad (1)$$

where $H_{w,e}$ equals $\sum_j A_{w,e,j}$ with $A_{w,e,j} = 0.5$ h if a provider is contracted and available to deliver the response throughout the j^{th} half-hour settlement period (SP) in the e^{th} block; otherwise, $A_{w,e,j} = 0$. The term K_w describing the provider's performance in the w^{th} week is converted from a percentage performance measure (PPM) over a random half-hour sample period within any contracted EFA block in the week by Table I. The PPM is the ratio between the aggregated spot values of FRs actually delivered and those that are required in the sample period [10].

TABLE I. CONVERSION FROM PPM TO PERFORMANCE FACTOR K_w

PPM	0% ~ 10%	10% ~ 60%	60% ~ 95%	95% ~ 100%
K_w	0	0.5	0.75	1

3) Weekly pay-as-clear auctions

The DLH is auctioned by 4-hourly EFA blocks in a service week starting Friday at 23:00. In each EFA block, tenders are accepted in the price order to minimise the clearing price [8]. Fig. 2 plots historic clearing prices in 42 blocks over each of the 52 weeks from 29/11/2019 to 26/11/2020 [24] along with the medians in each block. The DLH is shown to be procured at lower prices in blocks from 23:00 to 07:00 (e.g., blocks 1, 2, 7, and 8) and those from 11:00 to 15:00 (e.g., blocks 4 and 10).

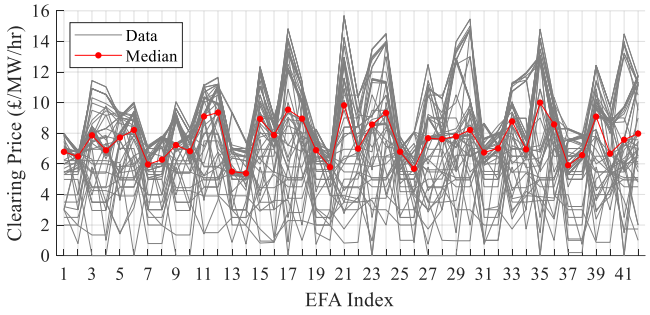

Fig. 2. Historic clearing prices of the DLH product in 42 EFA blocks over each of the 52 weeks from 29/11/2019 to 26/11/2020.

B. Bidding strategy in DLH Weekly Auctions

Evaluating the DLH payment for a service week based on the PPM in a random half-hour period presents a financial risk to a BESS provider which needs to follow the DLH curve (see Fig. 1) and thus has little chance to manage its SOC during the contracted EFA blocks. It is therefore necessary to leave some blocks untendered for the SOC restoration. Since a 4-hourly block expects to be sufficient to manage the SOC, the bidding strategy is designed to bid for a constant DLH capacity $P_{w,e}^{DLH}$ in the same amount of consecutive blocks N_{EFA}^{max} after each untendered block, starting from the first untendered block EFA_u. It is assumed here that all the tenders would be accepted by NGESO. Since the simulation found it difficult to achieve a profitable co-location project based on the median clearing price in each block of a week (see Fig. 2), twice the median prices are preliminarily adopted here as the DLH prices $\mathcal{P}_{w,e}^{DLH}$ in the optimisation, though the potential minimum tender price will be inferred from optimisation results in Section IV.D.

C. Non-Power-Exchange (NPE) Operating Strategy

In a NPE strategy, a BESS with power and energy capacities of P_B^R and C_B^R is co-located with a WF for the DLH provision and does not exchange energy with the WF, as shown in Fig. 3.

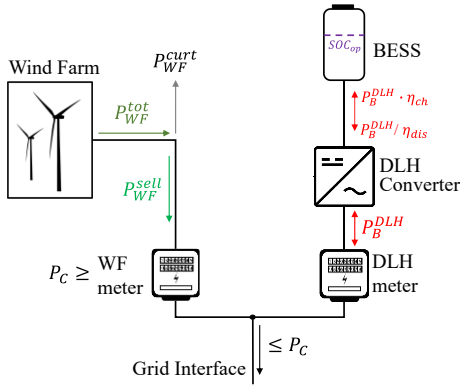

Fig. 3. The co-location system configuration for NPE operating strategy.

1) NPE operating strategy in tendered blocks

In tendered blocks, the BESS response P_B^{DLH1} is determined by the grid frequency using the DLH curve. When the BESS is close to an empty (or full) state, the required response might not be possible, i.e., drawing more energy than the available (or charging the BESS over the maximum limit). Therefore, P_B^{DLH1} of the BESS at a SOC level SOC_o is limited by Eq. (2).

$$|P_B^{DLH1}| \leq \begin{cases} \frac{C_B^{rm} \cdot (SOC_o - \underline{SOC})}{\Delta t / \eta_{dis}} & \forall P_B^{DLH1} > 0 \\ \frac{C_B^{rm} \cdot (\overline{SOC} - SOC_o)}{\Delta t \cdot \eta_{ch}} & \forall P_B^{DLH1} < 0 \end{cases} \quad (2)$$

where $\overline{SOC}$ and $\underline{SOC}$ are the maximum and minimum levels of SOC which are assumed here to be 100% and 0%; η_{dis} and η_{ch} are discharging and charging efficiencies respectively; Δt is the time step length used by the simulation; and C_B^{rm} denotes the remaining energy capacity (MWh) of the BESS which is daily updated based on the SOC time series over each day combined with a degradation model developed for a Li-Ion battery in [25] where the energy capacity loss is simulated by a combination of the calendar ageing and the cycle ageing. Then the SOC of the BESS is updated based on P_B^{DLH1}:

$$SOC_n = \begin{cases} SOC_o - \frac{P_B^{DLH1} \cdot \Delta t}{C_B^{rm} \cdot \eta_{dis}}, & \forall\ P_B^{DLH1} \geq 0 \\ SOC_o - \frac{P_B^{DLH1} \cdot \Delta t}{C_B^{rm} / \eta_{ch}}, & \forall\ P_B^{DLH1} < 0 \end{cases} \quad (3)$$

In this study, the power flow via WF meter is assumed to be limited by the available ampacity of the connection point only. In order to avoid high-frequency (HF) responses ($P_B^{DLH1} < 0$) unexpectedly coming from the exceedances of the available wind power P_{WF}^{tot} over the connection size P_C, i.e., the wind power to be curtailed, the wind power flowing across WF meter P_{WF}^{sell1} is additionally constrained by P_C:

$$P_{WF}^{sell1} = \min(P_{WF}^{tot},\ (P_C - P_B^{DLH1}),\ P_C) \tag{4}$$

2) NPE strategy in untendered blocks

In an untendered EFA block, the BESS is operated to restore its SOC to an optimal level SOC_{op}. Given $N_{\Delta t}$ time steps prior to the end of the block, if the BESS with $SOC_o > SOC_{op}$ can export $C_B^{o.op} = (SOC_o - SOC_{op}) \cdot C_B^{rm}$ during the remaining $(N_{\Delta t} - 1)$ time steps, the discharge power flowing to the AC grid via DLH meter P_B^{DLH0} in the present Δt is determined by the rise of P_C above P_{WF}^{tot} so as to avoid wind curtailment subject to $C_B^{o.op}$ and P_B^R. Otherwise, $C_B^{o.op}$ is evenly discharged across $N_{\Delta t}$ time steps. This is formulated by Eq. (5):

$$P_B^{DLH0} = \begin{cases} \min\left(\frac{\mathbb{O}(C_B^{o.op})\cdot\eta_{dis}}{\Delta t}, P_B^R, \mathbb{O}(P_C - P_{WF}^{tot})\right), & \forall \frac{C_B^{o.op}\cdot\eta_{dis}}{(N_{\Delta t}-1)\cdot\Delta t} \le P_B^R \\ \min\left(\frac{\mathbb{O}(C_B^{o.op})\cdot\eta_{dis}}{N_{\Delta t}\cdot\Delta t}, P_B^R\right), & \forall \frac{C_B^{o.op}\cdot\eta_{dis}}{(N_{\Delta t}-1)\cdot\Delta t} > P_B^R \end{cases} \tag{5}$$

where the operator $\mathbb{O}(\cdot)$ forces negative inputs to zero without affecting positive inputs. If $SOC_o < SOC_{op}$, the energy $C_B^{op.o} = (SOC_{op} - SOC_o) \cdot C_B^{rm}$ required for the SOC recovery will be evenly absorbed from the grid by P_B^{DLH0} across $N_{\Delta t}$ time steps. Then the wind power passing through WF meter P_{WF}^{sell0} and the new SOC are calculated by Eqs. (4) and (3) using P_B^{DLH0}.

D. Power-Exchange (PE) Operating Strategy

In a PE operating strategy, in addition to the DLH delivery, the BESS will be able to interchange energy with the WF via an additional converter (AdC) with a power capacity of $P_A^R \le P_B^R$ (see Fig. 4) so as to manage the SOC and assist in the time shift of wind generation (WG).

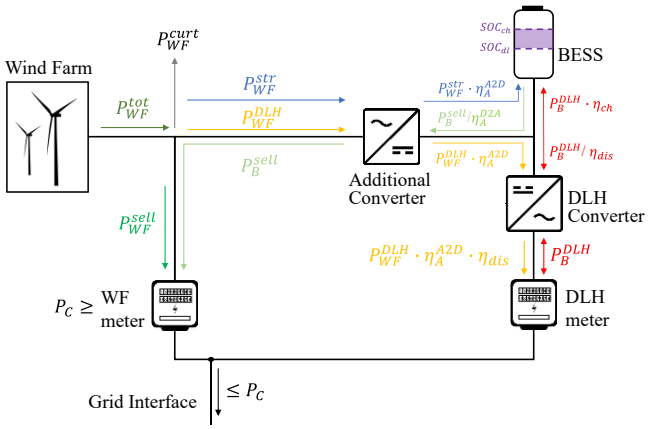

Fig. 4. The co-location system configuration for PE operating strategy.

1) PE strategy in tendered blocks

In tendered periods, the DLH delivery of the BESS P_B^{DLH1} is estimated from the grid frequency by the DLH curve subject to Eq. (2). If the BESS cannot offer the required low-frequency (LF) response P_{req}^{DLH}, i.e., $P_{req}^{DLH} > P_B^{DLH1} > 0$, the WF will assist the BESS in the DLH delivery by P_{WF}^{DLH} via the AdC subject to P_{WF}^{tot} and P_A^R (at a cost of the reduced WG-related revenue). The remaining wind power $(P_{WF}^{tot} - P_{WF}^{DLH})$ is then put onto the grid via WF meter subject to (i) the limit on WF meter determined by P_C and (ii) the remaining ampacity of the connection point $P_C^{AV} = (P_C - P_B^{DLH1} - P_{WF}^{DLH} \cdot \eta_A^{A2D} \cdot \eta_{dis})$ where η_A^{A2D} is the efficiency of the AdC rectifying AC to DC:

$$P_{WF}^{sell1} = \min(P_{WF}^{tot} - P_{WF}^{DLH},\ P_C^{AV},\ P_C) \tag{6}$$

A pair of SOC variables, i.e., $SOC_{dl} \le SOC_{ch}$, are used in this strategy to schedule the power exchange between WF and BESS. If the SOC after the delivery of P_B^{DLH1}, denoted by SOC_t, would be smaller than SOC_{ch}, the BESS will store the otherwise curtailed wind power P_{WF}^{str1} subject to $C_B^{ch.t} = (SOC_{ch} - SOC_t) \cdot C_B^{rm}$ and available power capacities of the BESS and the AdC; otherwise, the BESS does not absorb energy from the wind curtailment, avoiding an excessively high SOC level. This is formulated by Eq. (7).

$$P_{WF}^{str1} = \min\left(P_{WF}^{rm}, \frac{\mathbb{O}(C_B^{ch.t})}{\Delta t \cdot \eta_A^{A2D}}, \mathbb{B}^-(P_B^R, P_B^{DLH1}), (P_A^R - P_{WF}^{DLH})\right) \tag{7}$$

where $P_{WF}^{rm} = (P_{WF}^{tot} - P_{WF}^{DLH} - P_{WF}^{sell1})$ is the wind power to be curtailed and the operator $\mathbb{B}^-(\cdot)$ limits P_{WF}^{str1} by the available power capacity of the BESS which is also delivering P_B^{DLH1} [6].

For $SOC_t > SOC_{dl}$, the BESS transfers its surplus energy to WF meter via the AdC so as to restore its SOC while increasing the WG-related revenue associated with imbalance prices [26] in this study; otherwise, the BESS export to WF meter P_B^{sell1} is limited by 0 to keep the SOC from reducing to an excessively low level. P_B^{sell1} is also set to zero at times of $P_B^{DLH1} < 0$ so as to avoid any unexpected flow to the grid via WF meter of HF responses (which should be imported by the BESS). In a LF or deadband event (i.e., $P_B^{DLH1} \ge 0$), P_B^{sell1} is determined by $C_B^{t.dl} = (SOC_t - SOC_{dl}) \cdot C_B^{rm}$ subject to the available power capacities of connection point, BESS and AdC:

$$P_B^{sell1} = \min\left(\frac{\mathbb{O}(C_B^{t.dl})}{\Delta t/\eta_A^{D2A}}, (P_C^{AV} - P_{WF}^{sell1}), \mathbb{B}^+(P_B^R, P_B^{DLH1}), (P_A^R + P_{WF}^{DLH})\right),\ \forall P_B^{DLH1} \ge 0 \tag{8}$$

where η_A^{D2A} is the efficiency of the AdC converting DC to AC. (The efficiency-related terms are all assumed to be 0.95 in this study). The operator $\mathbb{B}^+(\cdot)$ limits P_B^{sell1} by the available power capacity of the BESS which is also delivering $P_B^{DLH1} \ge 0$ [6]. Then the SOC of the BESS is updated by:

$$SOC_n = \begin{cases} SOC_o - \frac{\left(P_B^{DLH1}/\eta_{dis} + P_B^{sell1}/\eta_A^{D2A} - P_{WF}^{str1}\cdot\eta_A^{A2D}\right)}{C_B^{rm}/\Delta t}, \forall P_B^{DLH1} \geq 0 \\ SOC_o - \frac{\left(P_B^{DLH1}\cdot\eta_{ch} + P_B^{sell1}/\eta_A^{D2A} - P_{WF}^{str1}\cdot\eta_A^{A2D}\right)}{C_B^{rm}/\Delta t}, \ \forall P_B^{DLH1} < 0 \end{cases} \quad (9)$$

2) PE strategy in untendered blocks

In an untendered block, the BESS is operated to restore its SOC to the region between SOC_{dl} and SOC_{ch} while reducing the WG curtailment. When $SOC_o < SOC_{ch}$ and $P_{WF}^{tot} > P_C$, the BESS can import the otherwise curtailed wind power P_{WF}^{str0} via the AdC subject to $C_B^{rm} \cdot (SOC_{ch} - SOC_o)$, $(P_{WF}^{tot} - P_C)$ and P_A^R. For $SOC_o > SOC_{dl}$ and $P_{WF}^{tot} < P_C$, the BESS discharges P_B^{sell0} through WF meter via the AdC under the constraints of $C_B^{rm} \cdot (SOC_o - SOC_{dl})$, $(P_C - P_{WF}^{tot})$ and P_A^R.

In the case that $SOC_o > SOC_{ch}$ or $SOC_o < SOC_{dl}$, the SOC is expected to reduce to SOC_{ch} or increase to SOC_{dl} before the end of the untendered block. If the BESS cannot export $C_B^{o.ch} = (SOC_o - SOC_{ch}) \cdot C_B^{rm}$ to or import $C_B^{dl.o} = (SOC_{dl} - SOC_o) \cdot C_B^{rm}$ from the grid via DLH meter over the remaining $(N_{\Delta t} - 1)$ time steps, it needs to additionally exchange power with the grid by P_B^{DLH0} in the present Δt even though $P_B^{DLH0} > 0$ may lead to the WG curtailment:

$$P_B^{DLH0} = \begin{cases} \mathbb{O}\left(\min\left(\frac{C_B^{o.ch}\cdot\eta_{dis}}{N_{\Delta t}\cdot\Delta t}, \ P_B^R\right) - P_B^{sell0}\right), \forall \frac{C_B^{o.ch}\cdot\eta_{dis}}{(N_{\Delta t}-1)\cdot\Delta t} > P_B^R \\ -\mathbb{O}\left(\min\left(\frac{C_B^{dl.o}/\eta_{ch}}{N_{\Delta t}\cdot\Delta t}, P_B^R\right) - P_{WF}^{str0}\right), \forall \frac{C_B^{dl.o}/\eta_{ch}}{(N_{\Delta t}-1)\cdot\Delta t} > P_B^R \end{cases} \quad (10)$$

Then the SOC is updated by Eq. (9) using P_B^{DLH0}, P_B^{sell0}, and P_{WF}^{str0}. The wind power flowing to the grid via WF meter P_{WF}^{sell0} is determined as the minimum of P_{WF}^{tot}, $(P_C - P_B^{sell0})$, or $(P_C - P_B^{sell0} - P_B^{DLH0})$.

III. Economic Optimisation by PSO Algorithm

A. DLH Availability Payment

The DLH availability payment R_w^{DLH} over a service week is estimated based on Eq. (1) through a comparison between the actual delivery and the required volume determined by the DLH curve. In order to mitigate the financial risk as noted in section II.B, the minimum of PPMs over all the sample periods within tendered blocks in a service week is selected here to evaluate the weekly performance factor K_w. In this way, the worst-case R_w^{DLH} will be considered in the optimisation process.

B. Green Subsidy

Given the export of a single WF being the minimum of P_{WF}^{tot} or P_C, co-locating the BESS with the WF for the DLH provision will affect the wind power flowing to the grid and the associated green subsidy. The Renewables Obligation (RO) scheme is one of the mechanisms supporting renewable generation in the UK [27]. The green subsidy price $\mathcal{P}_{RO}$ is approximated to be £100.1/MWh based on an assumption of 2 RO certificates (ROCs) being issued to each MWh of WG [27] combined with a buy-out price of £50.05/ROC for 2020/21 [28]. (In general, only the electricity generated by an accredited WF and supplied to customers, i.e., P_{WF}^{sell} in Figs. 3 and 4, can receive ROCs [29]). The variation of green subsidy δR_w^{RO} received by the WF owner after the BESS co-location in the w^{th} week is estimated by:

$$\delta R_w^{RO} = \sum_e \sum_j \mathcal{P}_{RO} \cdot \delta \overline{P}_{w,e,j}^{sell} \cdot 0.5 \text{ h} \quad (11)$$

where $\delta \overline{P}_{w,e,j}^{sell}$ denotes the average difference in P_{WF}^{sell} between the co-location system and a single WF during the j^{th} SP in the e^{th} block of the w^{th} week.

C. Energy Imbalance Charge

In the GB electricity market, a transmission-connected WF will pay (or be paid) for its net deficit (or surplus) of energy imbalance based on an imbalance price $\mathcal{P}_{w,e,j}^{EIC}$ (£/MWh) which reflects the cost of National Grid balancing the GB transmission system in each SP [26]. Therefore, the average difference in the power flow across WF meter $\delta \overline{P}_{w,e,j}^{WF}$ between the co-location system and a single WF is used to simulate the variation of the WF's energy imbalance charge (EIC) in a SP. According to [10], the average power flow across DLH meter $\overline{P}_{w,e,j}^{DLH}$ in a SP also causes EICs. Compared to a single WF, the EIC change δR_w^{EIC} after the BESS co-location in the w^{th} week is computed by:

$$\delta R_w^{EIC} = \sum_e \sum_j \mathcal{P}_{w,e,j}^{EIC} \cdot \left(\delta \overline{P}_{w,e,j}^{WF} + \overline{P}_{w,e,j}^{DLH}\right) \cdot 0.5 \text{ h} \quad (12)$$

D. BESS and Connection Costs

The capital expenditure (CAPEX) C_{CAPEX} of the co-located BESS mainly comprises costs of batteries and converters [6]. The unit prices of Li-Ion battery and converter are assumed here to be £166.4k/MWh and £85.8k/MW respectively according to [6]. The annual operational expense (OPEX) C_{OPEX} of the BESS is assumed to be 2% of C_{CAPEX} [6]. Co-locating a BESS to an existing transmission-connected WF in the GB will incur in connection costs (including an application fee) and influence the balancing services (BS) and transmission network (TN) use of system (UoS) charges. Since the transmission entry capacity is not changed in this study, the one-off application fee C_{APP} is around £26k based on the median base cost of the six connection zones [30]. Using the BSUoS price $\mathcal{P}_{w,e,j}^{BS}$ (£/MWh) assigned to each SP [31], the variation of BSUoS cost δC_w^{BS} in the w^{th} week after co-locating the BESS is computed from the average difference in the net electricity at the connection point in each SP of the week:

$$\delta C_w^{BS} = \sum_e \sum_j \mathcal{P}_{w,e,j}^{BS} \cdot \left|\delta \overline{P}_{w,e,j}^{WF} + \overline{P}_{w,e,j}^{DLH}\right| \cdot 0.5 \text{ h} \quad (13)$$

The TNUoS charges paid by generators for delivering their electricity over the GB TNs [32] depend on the generator's fuel type or the predominant type of a multi-fuel power plant under the current charging methodologies [3]. Since the predominant type of the co-location system explored here is intermittent, the annual TNUoS charge growth δC_{TN} due to the BESS operation

is determined by the increase of annual load factor (ALF) of the system. Given that an ALF of 10.8% would be used for a BESS prior to any historic data being available [32], the ALF of the WF+BESS system is assumed to increase by $10.8\% \times P_B^R/P_C$, resulting in $\delta C_{TN} = 919.6 \times P_B^R$ based on the TNUoS tariffs specified for a particular generation zone in 2019/2020 [32].

E. Particle Swarm Optimisation (PSO)

The PSO algorithm [33] is employed here to determine the co-located BESS size and strategy variables that maximise the net present value (NPV) of the project under each strategy. It optimises a problem starting from a set of random particles that travel in the search space until reaching convergence. For each particle that contains a vector of optimisation variables, power and energy flows across the system are simulated until C_B^{rm} falls below the retention limit of 80% [6] or cannot sustain the full response of DLH for the required 30 minutes. Since most of the monetary items are monthly billed [10], [32], present values of monthly cash flows are discounted by an annual return of 8% to compute the NPV:

$$NPV = -C_{CAPEX} - C_{APP} + \sum_m \frac{\sum_w (R_{m,w}^{DLH} + \delta R_{m,w}^{RO} + \delta R_{m,w}^{EIC} - \delta C_{m,w}^{BS}) - \delta C_m^{TN} - C_m^{OPEX}}{(1+8\%)^{m/12}} \quad (14)$$

where m is the index of calendar month starting from one; and C_m^{OPEX} and δC_m^{TN} in each month are presumed to be $C_{OPEX}/12$ and $\delta C_{TN}/12$ respectively. In the optimisation, the NPV of the system is maximised subject to technical requirements of DLH:

$$1\ \text{MW} \le P_{w,e}^{DLH} \le \min(50\ \text{MW}, P_B^R) \quad (15)$$

$$P_{w,e}^{DLH} \cdot 0.5\ \text{h} \cdot (\eta_{ch} + 1/\eta_{dis}) \le C_B^R \quad (16)$$

The PSO based modelling framework will be tested in the context of a particular 76 MW WF with P_C of 68.4 MW in the GB. (The source of wind farm information cannot be disclosed due to confidentiality). The 1-min average available powers of the WF and 1-sec grid frequencies [34] in the GB over 4 years from 2016 to 2019 are used to dispatch the outputs of the WF and its co-located BESS. The estimation of EICs and BSUoS charges are based on $\mathcal{P}_{w,e,j}^{EIC}$ [35] and $\mathcal{P}_{w,e,j}^{BS}$ [31] respectively in the same period.

IV. Optimisation and Simulation Results

The modelling of DLH bidding and operating strategies of co-location systems and the implementation of the PSO are all accomplished using MATLAB/Simulink [36]. The delivery of DLH service and the WF-BESS interaction will be simulated based on the optimised variables, followed by discussions of the profitability of co-locating BESS for the DLH delivery and the potential minimum tender prices in weekly auctions.

A. Optimisation Results

The optimised BESS size and variables used in bidding and operating strategies along with the resulting project timescale are listed in Table II for NPE and PE strategies, respectively. It is noted that the ordinary PSO algorithm employed here may fall in a local optimum or premature solution. However, given a large number of randomly initialised particles in this research, the same solutions have been obtained between different runs, suggesting that the global optimum could have been found in the search area.

TABLE II. The Optimal BESS Size and Strategy Variables

Variable	NPE	PE	Variable	NPE	PE
P_B^R (MW)	50	50	SOC_{op} (%)	46.78	n/a
C_B^R (MWh)	75.2	67.2	SOC_{dl} (%)	n/a	46.81
P_A^R (MW)	n/a	6.2	SOC_{ch} (%)	n/a	46.81
$P_{w,e}^{DLH}$ (MW)	50	50	EFA_u (-)	1	1
N_{EFA}^{max} (-)	2	2	Duration (yr)	9.62	9.13

The BESS MW capacity P_B^R is optimised to equal the DLH contract capacity $P_{w,e}^{DLH}$ which reaches the maximum allowable 50 MW [see Eq. (15)]. To ensure the DLH performance, the energy-to-power (E/P) ratio is optimised to be around 1.51 and 1.35 for NPE and PE respectively which are both greater than the minimum technical requirement as defined in Eq. (16) [i.e., $0.5 \times (\eta_{ch} + 1/\eta_{dis}) \approx 1.001$ in this case]. The PE leads to a smaller E/P ratio due to the 6.2 MW AdC placed between WF and BESS. This provides a path for the WF to support the DLH delivery when the co-located BESS has insufficient energy for low-frequency (LF) responses and also for the BESS to restore its SOC in tendered periods. For both NPE and PE, the optimal number of consecutive tendered EFA blocks is $N_{EFA}^{max} = 2$, with the first untendered EFA block $EFA_u = 1$. This means that the BESS should bid for the DLH provision in blocks over 03:00 – 11:00 and 15:00 – 23:00, most of which would be cleared at higher prices as was noted in Section II.A (see Fig. 2).

It is noted that SOC_{dl} and SOC_{ch} used in the PE strategy are optimised to be almost the same, meaning that there is little space for the WF-BESS interaction when the SOC reaches either SOC_{dl} or SOC_{ch}. In other words, there is less incentive to obtain the WG-related revenue from imbalance prices since the additional battery cycles between SOC_{dl} and SOC_{ch} would accelerate the battery degradation and thus reduce the duration of receiving payments from the DLH provision. Since the modelled battery degradation would reduce with a relatively smaller SOC [25], the optimal SOC level, i.e., 46.78% for NPE or 46.81% for PE, is slightly below 50%, resulting in a project timescale of around 9.62 or 9.13 years (i.e., 502 or 476 weeks) respectively while ensuring the DLH availability performance.

B. DLH Delivery and Availability Performance

The DLH delivery under the PE strategy and the PPM over each half-hour sample period in tendered EFA blocks within a particular week are shown in Fig. 5 with the gaps representing untendered blocks. The under-delivery around the simulation time of 1451.1h reduces the PPMs in the corresponding half-hour periods. The minimum PPM of about 97.65% is then used to derive the performance factor applied to the week based on Table I in order to mitigate the financial risk presented by the NGESO randomly adopting a sample period to assess the PPM for the whole week as was noted in Section II.B.

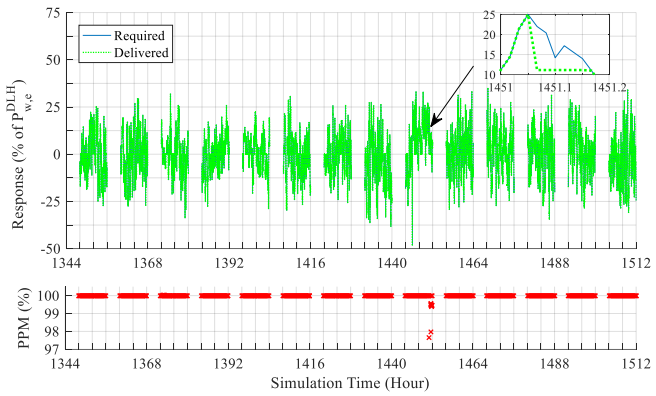

Fig. 5. The required and delivered responses (% of $P_{w,e}^{DLH}$) under the PE strategy and the PPM (%) over each half-hour sample period in tendered EFA blocks in a service week over 1344h-1512h (the gaps represent untendered blocks).

Fig. 6 shows distributions of the minimum PPMs of service weeks for NPE and PE respectively where the minimum PPMs exceed 95% (i.e., K_w = 1) in 95.02% and 90.76% of weeks and locate within 60% – 95% (i.e., K_w = 0.75) in 1.2% and 4.41% of weeks respectively. In addition, for the NPE, only 57 out of 112,480 half-hour SPs (i.e., 0.05%) within contracted blocks cannot receive the DLH payment due to the under-delivery of DLH causing $A_{w,e,j} = 0$ [see Eq. (1)]. For the PE, the under-delivery of DLH occurs in 135 out of 106,656 contracted SPs (i.e., 0.13%). The NPE having a higher E/P ratio shows a better availability performance on average than the PE at a cost of an increased investment in the BESS. It is noted that there are six or three weeks in NPE or PE respectively where the minimum PPM falling below 10% results in $K_w = 0$ and a full deduction in the DLH payment for the whole week [see Eq. (1)].

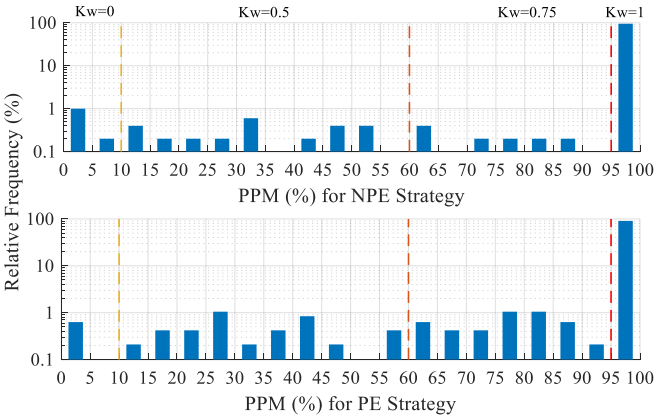

Fig. 6. Distributions of the weekly minimum PPMs for NPE and PE.

C. Coordination of WF and BESS

The outputs of WF and BESS coordinated by the NPE over nine particular blocks are shown in Fig. 7. In the untendered block over 1440-1444h, the exceedance of SOC over SOC_{op} is exported through DLH meter given the headroom in the power capacity of the common connection point. After the delivery of LF responses over 1446-1452h, the SOC decreases to a low level of 8.8%. In the subsequent untendered block, the BESS is constantly charged at around 7.39 MW to increase the SOC back to SOC_{op}. The LF responses provided by the BESS are also found to cause wind curtailment during high wind periods. As shown in the zoomed graphs in Fig. 7, when available wind power outputs P_{WF}^{tot} are close to the connection size P_C around 1504.7h, the WF has to curtail part of generation P_{WF}^{curt} so as to accommodate the LF delivery.

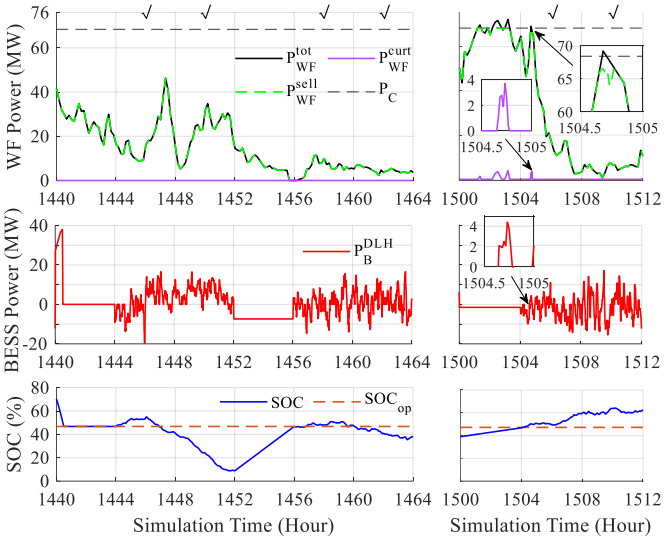

Fig. 7. Power outputs (MW) of WF and BESS coordinated by the NPE strategy and resulting SOC (%) in six EFA blocks over 1440-1464h and three blocks over 1500-1512h (the symbol √ denotes a tendered EFA block).

The coordination of WF and BESS in the PE and resulting SOC over the same nine blocks are shown in Fig. 8. Given the headroom in the connection point ampacity, the BESS with $SOC > SOC_{dl}$ exports its surplus energy through WF meter at P_B^{sell} via the 6.2 MW AdC either in an untendered block (e.g., around 1440h) or at times of $P_B^{DLH1} \geq 0$ in tendered blocks (e.g., around 1444.2h). The AdC also allows the BESS to absorb the otherwise curtailed wind power P_{WF}^{str} that coincides with $SOC < SOC_{ch}$. For example, the rise of P_{WF}^{tot} above P_C during 1502.2-1503.3h which would be curtailed in the NPE (see $P_{WF}^{curt} > 0$ in Fig. 7) is stored by the BESS via the AdC in the PE (see $P_{WF}^{str} > 0$ and $P_{WF}^{curt} = 0$ in Fig. 8), reducing the EIC of the BESS importing from the AC grid for its SOC recovery. In addition, the AdC enables the WF to assist the BESS in LF responses by delivering P_{WF}^{DLH} to DLH meter, e.g., over 1450.3-1451.6h where the SOC has decreased to 0% (see Fig. 8). Otherwise, the service unavailability for more than 1 h would incur in a zero PPM, leading to a full deduction in the DLH availability payment for the service week. In practice, a battery management system may prevent a BESS from discharging to a SOC level closer to 0%. The practical limits on the SOC can be reflected in the optimisation process through accordingly adjusting the values of $\underline{SOC}$ and $\overline{SOC}$ in Eq. (2).

It is noted that the ramp rate limits on BESS outputs are not incorporated into the modelling framework that focuses on the project's planning stage. In practice, the BESS import/export scheduled by operating strategies must be additionally adjusted to comply with the ramp rate limits under grid codes.

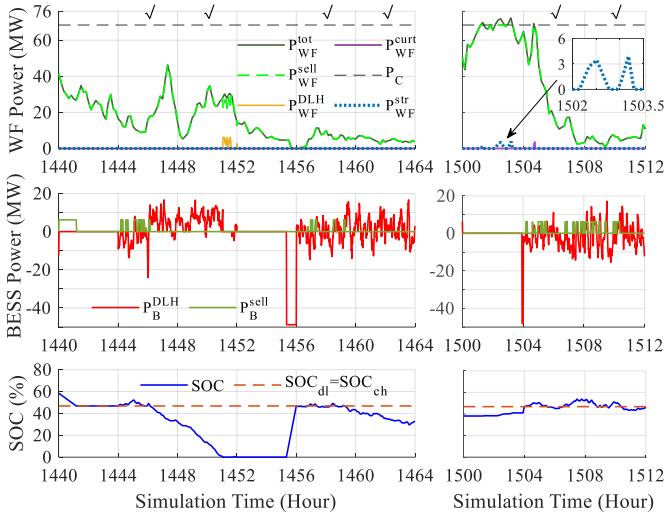

Fig. 8. Power outputs (MW) of WF and BESS coordinated by the PE strategy and resulting SOC (%) in six EFA blocks over 1440-1464h and three blocks over 1500-1512h (the symbol √ denotes a tendered EFA block).

D. System Profitability and Minimum Tendered Prices

The cumulative present values of monetary components of co-location systems simulated for NPE and PE based on the optimised variables are listed in Table III. Even though placing the 6.2 MW AdC causes additional costs, the decreased energy capacity of the BESS required by the PE (see Table II) results in smaller CAPEX and OPEX of the BESS than the NPE. In addition, compared to a single WF, the operation of the co-located BESS increases the TNUoS and BSUoS charges of the co-location system. For both NPE and PE, CAPEX and OPEX of the BESS contribute the most to the total system costs.

TABLE III. THE OPTIMISATION BASED CUMULATIVE PRESENT VALUES (£M) OF MONETARY ITEMS OF THE SYSTEMS UNDER NPE AND PE STRATEGIES

Item	NPE	PE	Item	NPE	PE
CAPEX	−16.806	−16.008	DLH Payment	30.783	29.320
OPEX	−2.798	−2.575	δEIC	−1.390	−1.084
App. Fee	−0.026	−0.026	δSubsidy (WF)	−1.150	−1.143
δTNUoS	−0.312	−0.301	**NPV**	**7.865**	**7.786**
δBSUoS	−0.435	−0.398	**IRR**	**20%**	**21%**

Since the BESS in the NPE gives a better DLH availability performance on average (see Fig. 6) and provides around half a year of DLH service more than the PE (see Table II), the total DLH payment in the NPE is greater than that in the PE. As was noted in Section IV.C, LF responses of the BESS could lead to wind curtailment in high wind periods. This not only reduces the green subsidy received by the WF, but also increases the EIC paid for the reduction of the power flow across WF meter compared to a single WF. In addition, due to the efficiency loss occurred in charging and discharging periods, the total energy absorbed by the BESS from the grid is greater than its injection into the grid via DLH meter. Therefore, the co-location system also needs to pay the EIC for the deficit of energy imbalance across DLH meter on average. In the PE, the BESS can store otherwise curtailed wind generation via the AdC for the SOC recovery (see Fig. 8), which reduces its import from the grid and leads to a smaller EIC than the NPE (see Table III).

In this study, similar NPVs and internal rates of return (IRR) are achieved between NPE and PE. Although the NPE leads to a slightly higher NPV, its IRR is smaller than the IRR in the PE due to a greater initial investment and a longer project timescale, meaning that the PE expects to be a more attractive option. It is noted that the DLH payment is estimated here based on twice the median of historic clearing prices in each EFA block of a service week. When DLH prices $\mathcal{P}_{w,e}^{DLH}$ are adjusted to around 1.46 times the median prices, the reduction in the total availability payment leads to a zero NPV in both NPE and PE. Therefore, given the particular WF and financial elements used in this study, the lowest tender prices in DLH weekly auctions are expected to be at least 146% of the median clearing prices which could ensure the profitability of the co-location project. In addition, the worst-case DLH payment has been evaluated here by selecting the minimum of PPMs over all half-hour sample periods within a service week. In practice, the PPM of a single random sample period will be adopted to determine the DLH performance for the whole service week. This means that the practical DLH availability payment will be greater than or equal to the payment simulated in this study.

V. CONCLUSIONS

The UK frequency response (FR) market reforms including the release of new FR products and the procurement by 4-houly blocks in weekly auctions incur in the need of evaluating the feasibility of a co-located wind farm (WF) and battery energy storage system (BESS) project under new circumstances. This paper has developed a modelling framework to optimise the co-located BESS size along with a set of strategy variables that are used to coordinate the WF and the BESS and specify the FR capacity and 4-hourly blocks to be tendered for the weekly auctioned Dynamic Low High (DLH) product. The proposed modelling framework has been tested based on a particular WF in the UK under different operating strategies.

The optimisation results indicate that co-location projects based on the particular WF would be profitable when the DLH price is at least 146% of the median of historic clearing prices in each block of a service week. Given the DLH prices being twice the median historic prices, the WF has been suggested to co-locate with a BESS that has an energy-to-power (E/P) ratio of around 1.5. The BESS is optimised to deliver a 50 MW DLH service for a maximum of two consecutive 4-hourly blocks and restores to a state of charge (SOC) level of about 46.8% in the subsequent untendered block. When an additional converter is used to enable the WF to assist the BESS in the low-frequency delivery and the SOC management, the best E/P ratio has been slightly decreased. This reduces the BESS lifetime and the net present value of the co-location system, but results in a slightly higher internal rate of return.

The modelling framework proposed here can be adapted to ancillary service markets in different countries by taking into

account the specific market mechanisms and requirements as well as local grid codes, connection charges and other revenue streams experienced by the onshore or offshore WF of interest. The modelling framework can be also applied to a WF under development by synthesising wind power time series based on its power curve and local wind data; the best transmission entry capacity (TEC) of the co-location system can also be estimated by integrating the TEC-dependent connection costs within the objective function. In addition, the varying financial elements (e.g., BESS unit prices and FR availability prices) could alter the trade-off between the BESS investment and its associated benefits. The investigation into the sensitivity of optimisation variables to key financial factors can assist in the determination of the optimal BESS capacity and strategy variables under the uncertainties of financial elements.

ACKNOWLEDGMENT

This work was conducted as part of the research programme of the Electrical Infrastructure Research Hub in collaboration with the Offshore Renewable Energy Catapult.

REFERENCES

[1] Upgrading Our Energy System: Smart Systems and Flexibility Plan, Office of Gas and Electricity Markets (Ofgem), London, UK, Jul. 2017.
[2] Electricity Storage and Renewables: Costs and Markets to 2030, Int. Renewable Energy Agency, Abu Dhabi, UAE, Oct. 2017.
[3] Introduction to Co-location, National Grid Electricity System Operator (NGESO), London, UK, Mar. 2019.
[4] F. Fan, I. Kockar, H. Xu, and J. Li, "Scheduling framework using dynamic optimal power flow for battery energy storage systems," *CSEE J. Power Energy Syst.*, vol. 8, no. 1, pp. 271-280, Jan. 2022.
[5] A. Michiorri, J. Lugaro, N. Siebert, R. Girard, and G. Kariniotakis, "Storage sizing for grid connected hybrid wind and storage power plants taking into account forecast errors autocorrelation," *Renewable Energy*, vol. 117, pp. 380-392, Mar. 2018.
[6] F. Fan, G. Zorzi, D. Campos-Gaona, G. Burt, O. Anaya-Lara, J. Nwobu, and A. Madariaga, "Sizing and coordination strategies of battery energy storage system co-located with wind farm: The UK perspective," *Energies*, vol. 14, no. 5, p. 1439, Mar. 2021.
[7] U. Akram, M. Nadarajah, R. Shah, and F. Milano, "A review on rapid responsive energy storage technologies for frequency regulation in modern power systems," *Renewable Sustain. Energy Rev.*, vol. 120, p. 109626, Mar. 2020.
[8] Future of Frequency Response Industry Update, NGESO, Feb. 2019.
[9] Response and Reserve Roadmap, NGESO, Dec. 2019.
[10] Response Auction Trial Service Terms (Phase 2), NGESO, Nov. 2019. https://www.nationalgrideso.com/document/159031/download
[11] V. Knap, S.K. Chaudhary, D.-I. Stroe, M. Swierczynski, B.-I. Craciun, and R. Teodorescu, "Sizing of an energy storage system for grid inertia response and primary frequency reserve," *IEEE Trans. Power Syst.*, vol. 31, no. 5, pp. 3447-3456, Sep. 2016.
[12] K.S. El-Bidairi, H.D. Nguyen, T.S. Mahmoud, S.D.G. Jayasinghe, and J.M. Guerrero, "Optimal sizing of battery energy storage systems for dynamic frequency control in an islanded microgrid: A case study of Flinders Island, Australia," *Energy*, vol. 195, p. 117059, Mar. 2020.
[13] T. Kerdphol, Y. Qudaih, and Y. Mitani, "Optimum battery energy storage system using PSO considering dynamic demand response for microgrids," *Int. J. Electr. Power Energy Syst.*, vol. 83, pp. 58-66, Dec. 2016.
[14] Y. Liu, W. Du, L. Xiao, H. Wang, and J. Cao, "A method for sizing energy storage system to increase wind penetration as limited by grid frequency deviations," *IEEE Trans. Power Syst.*, vol. 31, no. 1, pp. 729-737, Jan. 2016.
[15] J. Cao, W. Du, H. Wang, and M. McCulloch, "Optimal sizing and control strategies for hybrid storage system as limited by grid frequency deviations," *IEEE Trans. Power Syst.*, vol. 33, no. 5, pp. 5486-5495, Sep. 2018.
[16] P. Mercier, R. Cherkaoui, and A. Oudalov, "Optimizing a battery energy storage system for frequency control application in an isolated power system," *IEEE Trans. Power Syst.*, vol. 24, no. 3, pp. 1469-1476, Aug. 2009.
[17] D. Mejía-Giraldo, G. Velásquez-Gomez, N. Muñoz-Galeano, J.B. Cano-Quintero, and S. Lemos-Cano, "A BESS sizing strategy for primary frequency regulation support of solar photovoltaic plants," *Energies*, vol. 12, no. 2, p. 317, Jan. 2019.
[18] B. Lian, A. Sims, D. Yu, C. Wang, and R.W. Dunn, "Optimizing LiFePO4 battery energy storage systems for frequency response in the UK system," *IEEE Trans. Sustain. Energy*, vol. 8, no. 1, pp. 385-394, Jan. 2017.
[19] B. Xu, Y. Shi, D.S. Kirschen, and B. Zhang, "Optimal battery participation in frequency regulation markets," *IEEE Trans. Power Syst.*, vol. 33, no. 6, pp. 6715-6725, Nov. 2018.
[20] B. Cheng and W.B. Powell, "Co-optimizing battery storage for the frequency regulation and energy arbitrage using multi-scale dynamic programming," *IEEE Trans. Smart Grid*, vol. 9, no. 3, pp. 1997-2005, May 2018.
[21] S. Munoz-Vaca, C. Patsios, and P. Taylor, "Enhancing frequency response of wind farm using hybrid energy storage systems," in *Proc. the 5th Int. Conf. Renewable Energy Research Appl.*, Birmingham, UK, Nov. 2016, pp. 1-5.
[22] L. Johnston, F. Díaz-González, O. Gomis-Bellmunt, C. Corchero-García, and M. Cruz-Zambrano, "Methodology for the economic optimisation of energy storage systems for frequency support in wind power plants," *Appl. Energy*, vol. 137, pp. 660-669, Jan. 2015.
[23] J. Tan and Y. Zhang, "Coordinated control strategy of a battery energy storage system to support a wind power plant providing multi-timescale frequency ancillary services," *IEEE Trans. Sustain. Energy*, vol. 8, no. 3, pp. 1140-1153, Jul. 2017.
[24] NGESO, *Phase 2 auction trial, auction results*, 2020. https://www.nationalgrideso.com/balancing-services/frequency-response-services/frequency-auction-trial?market-information
[25] B. Xu, A. Oudalov, A. Ulbig, G. Andersson, and D.S. Kirschen, "Modeling of Lithium-Ion battery degradation for cell life assessment," *IEEE Trans. Smart Grid*, vol. 9, no. 2, pp. 1131-1140, Mar. 2018.
[26] The Electricity Trading Arrangements: A Beginner's Guide (Version 8), Elexon, London, UK, Feb. 2019.
[27] Renewables Obligation (RO): Guidance for generators that receive or would like to receive support under the Renewables Obligation (RO) scheme, Ofgem, Sep. 2018.
[28] Ofgem, *Renewables Obligation (RO) buy-out price and mutualisation ceilings for 2020-21*, 2020. https://www.ofgem.gov.uk/publications-and-updates/renewables-obligation-ro-buy-out-price-and-mutualisation-ceilings-2020-21
[29] Guidance for generators: Co-location of electricity storage facilities with renewable generation supported under the Renewables Obligation or Feed-in Tariff schemes (Version 3), Ofgem, Jul. 2020.
[30] NGESO, *Application Fee Calculator 19_20_0*, 2020. https://www.nationalgrideso.com/document/154976/download
[31] NGESO, *Balancing Services Use of System (BSUoS) Charges*, 2020. https://www.nationalgrideso.com/charging/balancing-services-use-system-bsuos-charges
[32] Final TNUoS Tariffs for 2019/20, NGESO, Jan. 2019. https://www.nationalgrideso.com/document/137351/download
[33] J. Kennedy and R. Eberhart, "Particle swarm optimization," in *Proc. Int. Conf. Neural Netw.*, Perth, Australia, Nov. 1995, pp. 1942-1948.
[34] NGESO, *Historic frequency data*, 2020. https://www.nationalgrideso.com/balancing-services/frequency-response-services/historic-frequency-data
[35] Elexon, *System sell & system buy prices*, 2020. https://www.bmreports.com/bmrs/?q=balancing/systemsellbuyprices
[36] MATLAB Release 2018b, The MathWorks, Inc., Mass., USA.